

DETECTION OF OPEN FRACTURES WITH VERTICAL SEISMIC PROFILING

by

W.B. Beydoun, C.H. Cheng and M.N. Toksöz

Earth Resources Laboratory
 Department of Earth, Atmospheric and Planetary Sciences
 Massachusetts Institute of Technology
 Cambridge, MA 02139.

ABSTRACT

In Vertical Seismic Profiling surveys tube waves are generated by compressional waves impinging on subsurface fractures or permeable zones. The problem of generation of these waves by a non-normal incident P wave for an inclined borehole intersecting a tilted parallel wall fracture is formulated theoretically. The amplitude of tube waves depends on the permeability, the length of the fracture, and on the frequency. The relative effects of these parameters are studied individually. The problem is also formulated for a thin oblate ellipsoidal (penny-shaped) fracture. The results for the two fracture models are compared and contrasted. Field data from Tyngsboro, Massachusetts are shown for open fractures in granite. From tube wave amplitudes normalized to P wave amplitudes, calculated permeabilities are on the order of one hundred millidarcys.

NOMENCLATURE

a^2	$K \mu^{-1} \gamma^{-1}$, pressure diffusivity in fracture
c	tube wave phase velocity
d	effective length of fracture
f	P wave or tube wave frequency
g	gravitational acceleration constant
$I_i(z), K_i(z)$	modified Bessel function of the i -th order
k	ω/c , tube wave vertical wavenumber
K	fracture permeability (1 darcy = $10^{-12} m^2$)
K_c	fracture hydraulic conductivity ($10^{-8} cm/sec$)
$L(t)$	fracture width
L_0	static fracture width
l	$k(1-c^2/\alpha^2)^{1/2}$, tube wave radial wavenumber from P wave contribution
m	$k(1-c^2/\beta^2)^{1/2}$, tube wave radial wavenumber from S wave contribution
n	$k(1-c^2/\alpha_f^2)^{1/2}$, tube wave radial wavenumber from fluid P wave contribution
\hat{n}	unit vector normal to the fracture walls
p^T	generated tube wave pressure amplitude in borehole fluid in the vicinity of the fracture
p^a	pressure amplitude in the borehole fluid of the first

$p(x,t)$	P wave arrival, in the vicinity of the fracture
P_0	fluid pressure distribution in the fracture
$q(x,t)$	equilibrium borehole pressure at fracture depth
$Q(t)$	rate of fluid flow in the fracture
r	pressure source function (inhomogeneous term) in PDE (A.2)
R	ellipsoidal fracture radius
\hat{s}	borehole radius
T	axis running along the center of the fracture, oriented away from the borehole
u	$1/f$, P wave or tube wave period
u_z^T	displacement amplitude along \hat{k} in the formation
V_{2D}	of the first P wave arrival, in the vicinity of the fracture
V	generated tube wave vertical displacement amplitude
V_0	along z_0 in the formation, in the vicinity of the fracture
\hat{Y}	two-dimensional volume of fluid ejected
\hat{z}_0	by the fracture in $T/2$
\hat{Z}	three-dimensional extrapolation of V_{2D}
α	total volume of fluid ejected by the ellipsoidal fracture
α_f	unit vector oriented $\hat{Z} \times \hat{s}$
β	unit vector along the borehole axis oriented downwards
γ	vertical unit vector oriented downwards
δ	compressional (P) wave velocity of the formation
Δ_f^T	compressional (P) wave velocity of the fluid
$\hat{\epsilon}$	shear (S) wave velocity of the formation
$\hat{\epsilon}^a$	fluid compressibility
$2\zeta_0$	$L_0/2r$, aspect ratio of ellipsoidal fracture
ϑ	$2\zeta_0/L_0$, maximum volumetric strain (or dilatation) of ellipsoidal fracture
\hat{k}	tube wave volumetric strain in the fluid
μ	maximum strain vector of the fracture
ρ	maximum strain vector of incident P wave
ρ_f	maximum normal fracture displacement
σ	$\cos^{-1}(\hat{k} \cdot \hat{n})$, angle between P wavenumber and fracture normal
φ	P wavenumber unit vector
Φ_f^T	dynamic fluid viscosity
χ	formation density
ω	fluid density
	Poisson's ratio of the formation
	$\cos^{-1}(\hat{n} \cdot \hat{z}_0)$, angle between borehole axis and fracture normal
	tube wave potential in the borehole fluid
	geometrical factor
	$2\pi f$, P wave or tube wave angular frequency

INTRODUCTION

Vertical Seismic Profiling (VSP) surveys have become a very valuable diagnostic tool in the evaluation of the formation properties surrounding the borehole. In field experiments with compressional wave VSPs, Huang and Hunter (1981a,b) had observed that tube waves are generated at fractures intersecting the borehole. In a similar set of experiments in Tyngsboro and in Hamilton, Massachusetts, we have observed the same phenomena. Examples of tube waves originating at fractures and propagating up and down the borehole

from the data collected at Tyngsboro and Hamilton are shown in a VSP section in Figures 1. and 2. The widely accepted mechanism for the generation of tube waves is that the incident P waves compress the fracture and inject a fluid pulse into the borehole. Figure 3 schematically illustrates this efficient mechanism for the generation of tube waves.

The fluid pulse mechanism for the generation of tube waves has been formulated mathematically by Beydoun *et al.* (1983). The geometrical model used in that study is that of a parallel-walled open fracture intersecting a borehole. A compressional plane wave impinges on the fracture. First, the volume of fluid ejected from the fracture into the borehole is calculated. Then, the tube wave amplitudes generated in the borehole fluid and in the formation are evaluated. Using this model, the *in situ* fracture permeability can then be estimated from the ratio of the tube wave amplitude to the P wave amplitude measured in the formation or in the fluid. The model used in Beydoun *et al.* (1983) assumed a vertical borehole, a horizontal fracture perpendicular to the borehole, and a vertical incident P wave normal to the fracture. In this paper we have extend this model to include random orientations of the borehole, fracture and the incident P wave. In addition, we have examined a fracture model based on a thin ellipsoidal (penny-shaped) crack. We will compare the theoretical predictions of the two models and the strengths and weaknesses of each. Finally, we will apply our parallel wall fracture model to the data from Tyngsboro.

THE PARALLEL WALL FRACTURE MODEL

The theory for the parallel wall fracture model has been discussed in some detail in Beydoun *et al.* (1983) for the vertical borehole, horizontal fracture and vertical incident P wave. In the following section, we will present the corresponding theory for the angle dependent model. The development is closely parallel to the original model, and we are presenting here the essential results that are different from the previous model. The reader is referred to Beydoun *et al.* (1983) for the more basic details.

Theory of Fluid Flow in the Fracture

Consider a parallel-walled, fluid-filled open fracture imbedded in a homogeneous isotropic elastic medium. The fracture is intersected by an uncased borehole. Let \hat{Z} be the vertical unit vector, let \hat{z}_b be the unit vector in the direction of the borehole axis, let \hat{n} be the unit vector normal the the fracture wall, and let \hat{s} be the axis normal to \hat{n} (parallel to the fracture walls and oriented away from the borehole) situated at the center of the fracture. These vectors and their origins are shown in Figure 4. The fluid in the fracture is in equilibrium with the fluid in the borehole. A plane P wave with wavenumber unit vector \hat{k} impinges on the fracture. For very small strains, the fracture width is assumed to oscillate about the static shape L_0 as

$$L(t) = L_0 - \zeta_0 \cos(\omega t) \quad (1)$$

where $2\zeta_0$ is the maximum normal fracture displacement.

To simplify the calculations of the fluid injection from the fracture into the borehole, the following assumptions are made: (1) $\zeta_0 \ll L_0$, (2) one-dimensional linear laminar regime of flow occurs within the fracture (Stokes' law satisfied), (3) the fluid compressibility is small, (4) the fluid injected into the borehole from the fracture does not significantly perturb the borehole pressure P_0 at the fracture location and the fracture pressure is equal to P_0 when the fracture velocity is zero, (5) low frequency approximation with frequency dependence ($\alpha T \gg R, L$), (6) the fracture intrinsic permeability, K , does not vary with time, (7) the fracture inclination with respect to the borehole axis $\varphi = \cos^{-1}(\hat{z}_b \cdot \hat{n})$ is small, and (8) if u is the maximum amplitude of the P wave particle displacement (along \hat{x}) in the vicinity of the fracture and $\vartheta = \cos^{-1}(\hat{x} \cdot \hat{n})$ the angle between the incident wave and the normal to the fracture, then for a thin fracture with large surface area and small fluid compressibility, $\zeta_0 \approx u \cos \vartheta$.

The two-dimensional problem, where the fracture is infinitely long in the Y direction, will be solved first. The fluid flow rate in the presence of a pressure gradient $\partial p(s, t) / \partial s$ is related to the fracture width $L(t)$, the fluid viscosity μ and density ρ_f , and the fracture intrinsic permeability K by Darcy's law (with Assumption (2), see for example De Wiest, 1969)

$$q(s, t) = - \frac{KL(t)}{\mu} \frac{\partial p(s, t)}{\partial s} \quad (2)$$

The elevation gradient term ($\rho_f g \partial Z / \partial s$) is not present because the fracture is plane and point-symmetric with respect to the z_b origin.

The fracture movement being T -periodic and $T/2$ symmetric, we shall investigate the fracture dynamics in a time interval of $T/2$ (from $t=0$ to $t=T/2$). The volume of fluid ejected from the fracture into the borehole (fracture closure) during the one-half cycle of the incident wave is (see Appendix A)

$$V_{2D}(K) = - \zeta_0 \left[\frac{K}{\pi \gamma \mu} \right]^{\frac{1}{2}} F(\omega, \zeta_0 / L_0) \quad (3)$$

where

$$F(\omega, \zeta_0 / L_0) \approx 2\omega \int_0^{T/2} (T/2 - t)^{\frac{1}{2}} \sin(\omega t) dt \quad \text{for } \zeta_0 \ll L_0.$$

An effective length of the fracture, d , can be defined as the radial distance (along \hat{s}) from the borehole wall to a point at which the pressure gradient falls to about ten percent the pressure gradient at the borehole wall over a time interval of $T/2$. The effective fracture length is given by the expression

$$d(K) = \left[\frac{2KT}{\mu \gamma} \right]^{\frac{1}{2}} \quad (4)$$

This can be verified by substituting Eq. (4) in Eq. (A.4) in Appendix A.

The volume used to derive Eq. (3) is two dimensional. The actual fracture geometry involves a three-dimensional configuration which can be approximated by extrapolation of the two-dimensional solution, assuming the geometry is axisymmetric with respect to the \vec{r} axis. This geometrical extrapolation is based on the steady state solution, and is assumed to be independent of the small fluid compressibility and of the low frequency of excitation.

Use of Navier-Stokes equation in cylindrical coordinates and the continuity equation (Landau and Lifchitz, 1971) with the assumptions (1), (2) and (5) indicate that the permeability of two-disc radial fluid flow is the same as the permeability of two parallel planes fluid flow. Comparing the steady state solutions for the 2D and 3D problems, the respectively flow rates can be related as follows:

$$q_{3D} = 2 \pi R \chi q_{2D} \quad (5)$$

where

$$\chi(K) = \frac{d(K)}{R \ln\left(\frac{R+d(K)}{R}\right)}$$

The χ component is defined as the geometrical factor; d is the effective fracture length defined previously in Eq. (4) and R is the borehole radius. For any given time interval the equation relating the two- and three-dimensional volumes is similar to Eq. (5), and in particular for a time interval of $T/2$

$$V(K) = 2 \pi R \chi(K) V_{2D}(K) \quad (6)$$

where V is the volume ejected from the circular fracture into the borehole during a time interval of $T/2$.

Tube Wave Generation

Tube waves are low frequency Stoneley waves. These guided waves reach their largest amplitudes at the solid-fluid boundary and decay approximately exponentially away from it. The fluid pulse V forced from the fracture into the borehole by an incident compressional wave generates tube waves which propagate up and down the borehole.

To determine the relationship between the ejected fluid volume and the tube waves generated, the tube wave volumetric strain (or dilatation) in the fluid (Δf) is used. Further, the tube wave and the P wave are assumed to have the same frequency. The integrated tube wave volumetric strain in the borehole fluid (at $z_b=0$) in the time period $T/2$ can be equated to the fluid volume injected into the borehole, $-V(K)$, over the same time period. The minus sign is necessary since the borehole system is different from the fracture system; the algebraic volume ejected from the fracture is a negative volume for the fracture but a positive volume for the borehole. In axisymmetric cylindrical coordinates this volume is expressed as

$$-V(K) = 2\pi c \int_0^{T/2} \int_0^R \Delta f^T(r, z_b=0, t) r dr dt \quad (7)$$

The volumetric strain and amplitude of the tube wave can be determined using the seismic potential for the tube wave (see Appendix B). The amplitudes of the up and down going tube waves will be the same because of symmetry.

The fracture permeability can be evaluated by considering the inverse problem. The *in situ* fracture permeability can be determined from the tube wave amplitude normalized to the direct P wave amplitude in the fluid (pressure ratio) or in the formation (displacement ratio). The P wave pressure in the borehole fluid can be written in terms of the displacement in the formation (White, 1965) with assumptions (5) and (8)

$$p^a / \zeta_0 = \frac{\omega \rho_f c^2 \alpha [1 - 2(\beta \cos(\varphi - \vartheta) / \alpha)^2] \cos(\varphi - \vartheta)}{\beta^2 [(1 - (c \cos(\varphi - \vartheta) / \alpha)^2) \cos \vartheta]} \quad (8)$$

where $\varphi - \vartheta = \cos^{-1}(\hat{k} \cdot \hat{z}_b)$ (oriented angles, see Figure 4.) is the angle between the P wavenumber vector and the borehole axis.

Using Eq. (B.2) to (B.8), the ratios of fracture induced tube wave amplitudes to incident P wave amplitudes can be determined. The pressure ratio in the borehole (measured by a hydrophone) is

$$p^T / p^a = C \frac{\omega \beta^2 \cos \vartheta [1 - (c \cos(\varphi - \vartheta) / \alpha)^2] I_0(nR)}{\zeta_0 \cos(\varphi - \vartheta) c^2 \alpha [1 - 2(\beta \cos(\varphi - \vartheta) / \alpha)^2]} \quad (9)$$

where $C = C(K)$ is given in equation (B.8).

The component along z_b of the displacement ratio at the wall of the borehole (measured by an anchored borehole geophone) is

$$u_z^T / (u \cos(\varphi - \vartheta)) = [kK_0(lR) + mGK_0(mR)] A \cos \vartheta / (\zeta_0 \cos(\varphi - \vartheta)). \quad (10)$$

The factor A is related to C by Eq. (B.5), and C is related to the fracture flow via Eq. (B.8). Eq. (9) or (10) can be solved to determine the fracture permeability K . Normally, given the formation and fluid properties, displacement or pressure ratios can be determined as a function of frequency with permeability, K , as a parameter. These values can then be compared with observations to determine K .

A simple relation exists between the fracture intrinsic permeability K and the fracture hydraulic conductivity (or coefficient of permeability) K_c

$$K_c = K \rho_f g / \mu. \quad (11)$$

The SI units of K are m^2 , and the common unit is the darcy ($1 d = 10^{-12} m^2$). The SI units of K_c are m/sec , and the common unit is $10^{-3} cm/sec$, which is sometimes called the darcy; to avoid any confusion this nomenclature shall not

be used. However if the fluid is water a simple approximate relation exists :
 1 darcy $\approx 10^{-3}$ cm/sec.

ELLIPTICAL FRACTURE MODEL

In order to study the model dependence of our results, we need to study different models of fractures. One such model is the elliptic or penny-shaped crack model of the fracture. In this model, the fracture is assumed to be circular, with the fracture height very much smaller than the fracture radius. We also assume that the borehole is located at the center of the fracture, that its radius is small compared to the fracture radius and that it acts as an infinite drain for the fluid ejected from the fracture. In that sense, the fracture can be treated to be under the "drained" condition. Other assumptions are: the wavelength of the incident wave is much longer than the size of the fracture; the frequency of excitation is low enough for complete drainage from the fracture during any stress cycle; and the incident strain is small enough that the fracture is never completely closed.

Under these conditions, the volumetric strain of the fracture is related to the applied strain using the theory of Eshelby (1957). The volumetric strain of the fracture can then be related to the volume of fluid ejected and compared with that obtained using the previous model. The applied strain can be related to the incident displacement. In this way we can relate the incident P wave displacement to the volume of fluid ejected from the fracture into the borehole in a manner similar to that given in Eq. (6).

Theory

Without loss of generality, we can assume the fracture to be horizontal and the borehole to be vertical. An incident P wave impinges on the fracture at an angle ϑ with the normal to the fracture. Using the same coordinate system as in Figure 4., the maximum dilatational strains of the incident P wave are defined as ε_{xx}^a and ε_{zz}^a . If the boundary conditions are written in terms of maximum stresses, we can infer the maximum strains from the constitutive relation of the medium. The incident strain vector (composed of the three maximum dilatational components of the strain tensor), $\vec{\varepsilon}^a$, can be related to the strain vector of the fracture, $\vec{\varepsilon}$, by the matrix equation (Eshelby, 1957; Anderson *et al.*, 1974; Cheng, 1978):

$$\vec{\varepsilon} = A \vec{\varepsilon}^a, \quad (12)$$

where A is the strain enhancement factor (Korringa *et al.*, 1979). For low aspect ratio (thin) fractures, results show that only ε_{zz}^a is important in the calculation of the volumetric strain of the fracture. The maximum volumetric strain Δ of the fracture is given by:

$$\Delta = \frac{4(1-\sigma)^2}{\pi\delta(1-2\sigma)} \varepsilon_{zz}^a, \quad (13)$$

where σ is Poisson's ratio of the formation and δ is the aspect ratio of the fracture (width divided by diameter). From the notations of the parallel wall model, we have $\delta = L_0/2r$ and $\Delta = 2\zeta_0/L_0$. Therefore, the elasticity effects of the medium, ignored in the parallel wall model, can be taken into account since

equation (13) links ζ_0 to the boundary conditions in the elastic medium. In the "drained" case under consideration, the volume of fluid ejected can be assumed to be the volumetric strain of the fracture multiplied by the (negative) fracture volume. The volume of an ellipsoidal fracture with radius r and aspect ratio δ is $4\pi\delta r^3/3$. Thus, the volume ejected into the borehole upon an incident P wave at an angle ϑ with the normal to the fracture is given by:

$$V_e = -\frac{4}{3}\pi r^2 \zeta_0 \quad (14)$$

Identifying this volume, V_e , with the volume V given by equation (6), an expression for the ellipsoidal fracture radius, r , is found:

$$r = \left(\frac{-3V}{4\pi\zeta_0} \right)^{1/2} \quad (15)$$

Note that $-V$ is a positive quantity (see Eq. 3).

Comparison with Parallel Wall Model

The parameters of comparison are the effective fracture distance, d , versus the ellipsoidal fracture radius, r . The variables considered are the frequency and the fracture permeability. The other physical parameters are kept constant and their values are shown in Table 1. Results are shown in the table below:

		$d(m)$	$r(m)$
$f=150$ Hz,	$K=10$ d	0.52	0.41
$f=100$ Hz,	$K=10$ d	0.63	0.48
$f=50$ Hz,	$K=10$ d	0.89	0.64
$f=150$ Hz,	$K=1$ d	0.16	0.18
$f=100$ Hz,	$K=1$ d	0.20	0.21
$f=50$ Hz,	$K=1$ d	0.28	0.29

These results compare favorably in the sense that they are of the same order of magnitude, considering that the two models presented in this paper are based on totally different approaches. The effective fracture length is comparable to the radius of the ellipsoidal fracture.

There is no dependence on formation properties in the parallel wall model. The main interest was, that assuming the displacement field in the vicinity of the fracture, to calculate the maximum volume of fluid ejected by the fracture, the fluid properties being taken into account. Formation properties can be approximately incorporated by specifying the boundary conditions of the incident field and using Eq. (13).

There is no dependence on the fluid properties in the ellipsoidal crack model. This is because we have used the "drained" assumption. Fluid properties, both elastic and viscous, can be incorporated into the ellipsoidal

crack model (Johnston *et al.*, 1979). Furthermore, the borehole radius effect is not present in the formulation since we have assumed the borehole radius to be small compared to r . However, when the borehole radius is decreased by a factor of 10 (from 0.1m to 0.01m), the fracture radius calculated using Eq. (15) is decreased by approximately 30 percent. Therefore, the borehole effect does not significantly change the results. Frequency dependence, as used in the parallel wall fracture model, can also be introduced into the ellipsoidal model, provided the long wavelength assumption still holds (Kuster and Toksöz, 1974).

It is clear that for both models, given the observed P wave to tube wave pressure ratio, one can obtain only one parameter for the fracture. In the case of the parallel wall fracture model, the parameter is the width of the fracture, and by inference, the *in situ* fracture permeability. On the other hand, in the case of the ellipsoidal fracture model, the parameter one can obtain is the radius of the fracture. Comparison of the two models brings additional information. The two main consequences of this comparison are: the parallel wall model can be extended to include formation properties in the calculation of the volume V and the fracture effective distance is representative of the fracture radius.

RESULTS AND DISCUSSION

In order to demonstrate the different efficiencies of tube wave generation, three separate formations are considered: a granite, representing a typical crystalline rock; a "hard" sediment that would represent relatively dense carbonate and hard sandstones; and a "sediment" to represent the more typical sedimentary rocks such as sandstones and shales. The properties of these formations and other physical parameters used in this study are listed in Table 1. The tube wave phase velocity c is calculated by solving the tube wave period equation for the given formation and borehole parameters as a function of frequency.

Before we discuss specific numerical and field results, there are several points of interest that are apparent from a close examination of the analytic expressions for the fluid ejection and tube wave generation. These are discussed briefly as follows:

For a given fracture permeability, formation and P wave angle of incidence a smaller borehole radius gives a higher p^T/p^a ratio. This is related to the χ factor in the extension from the two-dimensional model to three dimensions.

For the case where the borehole is vertical and the incident P wave is also vertical, the fracture inclination being ϑ , we can observe from Eq. (B.8) that $C(K)$ is a monotonically increasing function of the permeability K . Then p^T/p^a in Eq. (9) is proportional to $C(K) \cdot \cos\vartheta$. Therefore if ϑ is unknown, and we wish to have an estimate of K given p^T/p^a , then setting $\vartheta=0$ will yield a lower bound for K .

The tube wave to P wave pressure ratio p^T/p^a is maximum for ϑ minimum and minimum for ϑ maximum. Therefore by rotating the the source around the borehole, one can estimate the inclination of the fracture plane.

Pressure and Displacement Amplitude Ratios

The ratios of tube wave amplitudes to P wave amplitudes are shown in Figures 5 - 8 for the simple case where $\vartheta = \varphi = 0$. The first comparison made is that of the ratios of pressure amplitudes inside the borehole fluid. This is useful for interpreting the hydrophone data. The second comparison is that of the ratios of displacements that may be measured by a borehole seismometer locked to the borehole wall. Only the component of the displacement along z_b is considered. The tube wave particle motion at the borehole interface is highly elliptical and it is important to specify the component of displacement under consideration. Owing to the much larger amplitudes of tube waves in the fluid it is preferable to use hydrophone data as opposed to geophone data to detect highly permeable zones. The borehole acts essentially as an amplifier. The tube wave pressure amplitudes in the fluid diminish with increasing frequency. The displacement ratios in the formation increase with frequency. Higher fracture permeability yields higher tube wave amplitudes. For a given fracture permeability, the "harder" the formation is, the higher the tube wave pressure amplitude in the fluid (Figure 5a, 6a, and 7a), and the lower the tube wave displacement amplitude in the formation (Figure 5b, 6b and 7b).

Figure 8 shows the effect of the borehole radius on the TW/PW pressure ratio. When the radius decreases the fluid volume decreases and, for a constant fracture permeability, the TW/PW ratio balances this decrease by increasing (Eqs. 9, B.8 and 6).

Field Examples

Field examples of tube wave generation in a borehole which intersects open fractures in granite are shown in Figures 1. (Tyngsboro, Mass.) and 2. (Hamilton, Mass.). These examples are pressure measurements in the borehole fluid. Comparison of data from the televiwer and the tube waves show a good correlation between tube wave generation and open fractures.

For the Tyngsboro data, the tube wave to P wave amplitude ratios were calculated as a function of frequency in well #3 for three fracture depths: 253', 290' and 471'. Due to weak P wave signals these values have relatively large error bars (in average about ± 3 in the TW/PW ratio). These values are superimposed on the theoretical iso-permeability curves of a granite model with a borehole radius of 7.6 cm with $\vartheta = \varphi = 0$ (Figure 9). The trend of the data follows in some sense the theoretical curves. The permeability ranges between approximately 0.1 and 0.5 Darcys. These values are consistent with other permeability calculations in fractured granite as compiled by Brace (1980).

However, preliminary comparisons between the observed flow and the estimated flow (calculated from the theoretical permeability, an estimated fractured zone width and a pressure head) show that the the estimated flow is lower than the observed one. This could be due (by order of importance) to (1) an over-estimate of the effective fracture distance; which means that only a part of the distance contributes to the volume ejected, therefore, a smaller volume is ejected for an observed TW/PW ratio; (2) an inclined fracture for which, if the model is used with $\vartheta = 0$, would yield a lower bound of the permeability, thus, a lower flow; and (3) the perhaps inaccurate assumption of linear laminar regime of flow; this would yield a lower volume ejected and a

lower estimated fracture permeability. More field data are being processed at the present time and the results will be further compared with those obtained from the model. This will be the subject of an forthcoming paper.

CONCLUSIONS

Tube waves can be used to detect open fractures intersecting a borehole and to determine an equivalent fracture permeability using tube wave to P wave amplitude ratios in the borehole fluid (pressure ratio). It should be noted that the tube to P wave pressure ratio in the borehole fluid is approximately 3 orders of magnitude greater than the displacement ratio in the formation. For this reason it is preferable to use hydrophone data instead of wall-locked borehole geophone data, to locate these permeable zones. It is important to mention that a number of assumptions were made in this study and a complex "equivalency" was established between the two-dimensional cartesian geometry and the circular crack model. Another fracture model based on the static compression of an thin ellipsoidal or penny-shaped crack was developed. The comparison shows that the fracture effective distance is representative of the fracture radius. The parallel wall fracture model was applied to VSP data from Tyngsboro and Hamilton, Massachusetts. The results show a reasonable agreement with data.

ACKNOWLEDGMENT

The authors would like to thank Ernest Hardin from MIT/ERL for the processing and display of the data. This research was partially supported by the Full Waveform Acoustic Logging Consortium at M.I.T.

REFERENCES

- Beydoun, W.B., Cheng, C.H. and Toksöz, M.N., 1983, Detection of Subsurface Fractures and Permeable Zones by the Analysis of Tube Waves: Annual Report FWAL consortium, MIT/ERL.
- Brace, W.F., 1980, Permeability of crystalline and argillaceous rocks: Int. J. Rock Mech. Min. Sci. & Geomech. Abstr., v.17, p.241-251.
- Cheng, C.H., 1978, Seismic velocities in porous rocks direct and inverse problems: Sc.D. thesis, M.I.T., Cambridge.
- Cheng, C.H. and Toksöz, M.N., 1981, Elastic wave propagation in a fluid-filled borehole and synthetic acoustic logs: Geophysics, v.46, p.1042-1053.
- De Wiest, R.J.M., 1969, Flow Through Porous Media: Academic Press, New York.
- Eshelby, J.D., 1957, The determination of the elastic field of an ellipsoidal inclusion, and related problems: Proc. Roy. Soc. London, Ser. A, v.241, p.376-396.

- Huang, C.F. and Hunter, J.A., 1981a, The correlation of "tube wave" events with open fractures in fluid-filled boreholes: Current Research, Part A, Geological Survey of Canada, Paper 81-1A, p.361-376.
- _____, 1981b, A seismic "Tube Wave" method for in-situ estimation of fracture permeability in boreholes: S.E.G. Preprint Series, 51st Annual International Meeting, Los Angeles, v.1, E1.4 p.23-46.
- Johnston, D.H., Toksöz, M.N. and Timur, A., 1979, Attenuation of seismic waves in dry and saturated rocks, II. mechanisms: Geophysics, v.44, p.691-711.
- Korringa, J., Brown, R.J.S., Thompson, D.D. and Runge, R.J., 1979, Self-consistent imbedding and the ellipsoidal model for porous rocks: J. Geophys. Res., v.84, p.5591-5598.
- Kuster, G.T. and Toksöz, M.N., 1974, Velocity and attenuation of seismic waves in two-phase media: Part I. theoretical formulations: Geophysics, v.39, p.587-606.
- Landau, L. and Lifchitz, E., 1976, Mécanique des Fluides, MIR Publications, Moscow.
- White, J.E., 1965, Seismic Waves, Radiation, Transmission and Attenuation; McGraw Hill Book Company.

Table 1. Physical parameters used in this study

Formation	$\alpha(m/s)$	$\beta(m/s)$	$\rho(kg/m^3)$
granite	5500	3300	2700
"hard"	4500	2500	2300
"sediment"	3000	1200	2100
fluid	1500	0	1000
fluid viscosity	μ	$= 10^{-3}$	Poiseuilles
fluid incompressibility	γ^{-1}	$= 2 \cdot 10^9$	Pa
borehole radius	R	$= 0.1$	m

APPENDIX A: TWO-DIMENSIONAL SOLUTION OF FRACTURE FLOW

The volume of fluid ejected from the fracture into the borehole (fracture closure) in $T/2$ is derived from the calculation of the injected fluid volume from the borehole to the fracture (fracture opening) in $T/2$. The net change of fluid dq in a volume element $L(t)ds$ is due to the volume of fluid injected into the fracture (fracture opening) and the compressibility of the fluid (no mass is generated or lost in the element). During a time increment dt , this total change is

$$-dq dt = \frac{dL(t)}{dt} dsdt + L(t)\gamma \frac{\partial p(s,t)}{\partial t} dsdt \quad (\text{A.1})$$

where γ is the fluid compressibility and $dL(t)/dt = \omega\xi_0 \sin(\omega t)$, the velocity of the fracture wall. The net storage given by (A.1) must equal the net volume of fluid $(\partial q(s,t)/\partial s) dsdt$ flowing into the differential volume, giving

$$\frac{\partial}{\partial s} \left[\frac{K}{\mu} L(t) \frac{\partial p(s,t)}{\partial s} \right] = L(t)\gamma \frac{\partial p(s,t)}{\partial t} + \frac{dL(t)}{dt}$$

Setting $\alpha^2 = K/\mu\gamma$ and $Q(t) = \omega\xi_0 \sin(\omega t)/(\gamma L(t))$, the following equation is found

$$\alpha^2 \frac{\partial^2 p(s,t)}{\partial s^2} - \frac{\partial p(s,t)}{\partial t} = Q(t) \quad (\text{A.2})$$

with the boundary conditions for pressure (Assumption (4))

$$\begin{aligned} p(s=R,t) &= P_0 & \text{for all } t \geq 0 \\ p(s,t=0) &= P_0 & \text{for all } s \geq R \\ \partial p(s,t)/\partial s &= 0 & s \rightarrow \infty \end{aligned}$$

Eq. (A.2) is a one-dimensional inhomogeneous diffusion equation. The heat conduction analogy corresponds to a semi-infinite half-space ($s \geq R$) having α^2 as thermal diffusivity and a time varying heat source $Q(t)$. The second condition assumes that the diffusion process is over before $T/2$, since the process is reversed every $T/2$. The last condition states that there is no fluid flow in the fracture far ($s \gg R+d$) from the borehole intersection.

The solution to this partial differential Eq. (A.2) is found by the standard Laplace transform method

$$p(s,t) = P_0 - \int_0^t Q(\tau) \operatorname{erf} \left[\frac{(s-R)}{2\alpha(t-\tau)^{1/2}} \right] d\tau \quad s \geq R \quad (\text{A.3})$$

where $\operatorname{erf}(z) = \frac{2}{\sqrt{\pi}} \int_0^z e^{-\xi^2} d\xi$ is the error function.

Thus, the pressure gradient is

$$\frac{\partial p(s,t)}{\partial s} = -\frac{1}{\alpha\sqrt{\pi}} \int_0^t Q(\tau) \exp\left[\frac{-(s-R)^2}{4\alpha^2(t-\tau)}\right] (t-\tau)^{-1/2} d\tau \quad s \geq R \quad (\text{A.4})$$

The rate at which fluid flows is given by Eq. (2). By calculating the volume injected into the fracture for the maximum fracture displacement $2\xi_0$, we can obtain the maximum volume injected in a finite amount of time. This maximum volume occurs during a time interval of $t = T/2$. Therefore the volume of fluid forced into the fracture from the borehole in $T/2$ is

$$V_{2D} = \int_0^{T/2} q(s=R,t) dt$$

or explicitly,

$$V_{2D}(K) = \xi_0 \left[\frac{K}{\pi\gamma\mu} \right]^{1/2} F(\omega, \xi_0/L_0) \quad (\text{A.5})$$

where

$$F(\omega, \xi_0/L_0) = \omega \int_0^{T/2} \int_0^t \frac{1 - (\xi_0/L_0)\cos(\omega t)}{1 - (\xi_0/L_0)\cos(\omega\tau)} \frac{\sin(\omega\tau)}{(t-\tau)^{1/2}} d\tau dt$$

Since $L(t)$ is T -periodic and $T/2$ -symmetric we can directly infer from (A.5) the fluid volume forced from the fracture into the borehole. The right hand side of (A.5) is different in sign during the fracture closure, because the fluid flows in the opposite direction. Therefore the volume of fluid injected into the borehole in $T/2$ is given by Eq. (3).

Computation shows that for increasing frequency, $F(\omega, \xi_0/L_0)$ decreases. As the frequency increases less fluid is ejected into the borehole. For $\xi_0 \ll L_0$ (Assumption (1)), an asymptotic expression for F can be found by interchanging the order of integration in the (τ, t) plane:

$$F(\omega, 0) = 2\omega \int_0^{T/2} (T/2-t)^{1/2} \sin(\omega t) dt$$

APPENDIX B: TUBE WAVE SOURCE

The borehole geometry is taken to be axi-symmetric with respect to the z_b axis. The generated tube wave potential in the fluid is chosen to be

$$\Phi_f^T(r, z_b, t) = C I_0(nr) \sin[\omega t - kz_b] \quad r \leq R^- \quad (\text{B.1})$$

where C is a parameter, depending on the medium and the fluid properties. In this problem, C will depend also on the fracture parameters.

The tube wave pressure amplitude in the borehole fluid p^T and its displacement amplitude in the formation along z_b , u_z^T , are then given by, ignoring the sinusoidal time dependence for the moment:

$$p^T = \rho_f \omega^2 C I_0(nr) \quad r \leq R^- \quad (\text{B.2})$$

$$u_z^T = A [kK_0(lr) + mGK_0(mr)] \quad r \geq R^+ \quad (\text{B.3})$$

where

$$G = \frac{2l\beta^2 K_1(lR)}{k(c^2 - 2\beta^2) K_1(mR)} \quad (\text{B.4})$$

$$A = \frac{C n I_1(nR) (2\beta^2 - c^2)}{l c^2 K_1(lR)} \quad (\text{B.5})$$

Tube wave volumetric strain in the fluid is defined as

$$\Delta_f^T = \partial u_{fr}^T / \partial r + u_{fr}^T / r + \partial u_{fz}^T / \partial z_b$$

where u_{fr}^T and u_{fz}^T are the radial (perpendicular to z_b) component and the component along z_b of the tube wave particle displacement in the fluid.

The relations between the potential and the displacement components are

$$u_{fr}^T = \partial \Phi_f^T / \partial r \quad \text{and} \quad u_{fz}^T = \partial \Phi_f^T / \partial z_b$$

Therefore a simple relation arises between the volumetric strain and the potential

$$\Delta_f^T = \nabla^2 \Phi_f^T \quad (\text{B.6})$$

where ∇^2 is the Laplacian operator. Calculation of Eq. (B.6) with (B.1) yields

$$\Delta_f^T(r, z_b, t) = C (c^2 / \alpha_f^2 - 2) k^2 I_0(nr) \sin[\omega t - kz_b] \quad (\text{B.7})$$

The double integral in (7) is easily computed, since the variables are separated

$$-V(K) = 4\pi R C(K) (2 - c^2/\alpha_f^2) I_1(nR) k/n$$

The parameter C depends on the fracture parameters and therefore couples the fracture movement to the tube wave propagation. The tube wave pressure in the fluid and displacement in the formation are now linked to the fracture dynamics (Eq. (B.2) and (B.3)). Using Eq. (6) and (3) we finally obtain

$$C(K) = \zeta_0 \chi(K) \left(\frac{K}{\pi\gamma\mu} \right)^{1/2} F(\omega, \zeta_0/L_0) \frac{(1 - c^2/\alpha_f^2)^{1/2}}{2(2 - c^2/\alpha_f^2) I_1(nR)} \quad (\text{B.8})$$

TYNGSBORO WELL No. 2
WEIGHT DROP SOURCE, OFFSET B3
BANDPASS FILTERED (60 - 200 Hz)
TRACE AMPLITUDE NORMALIZATION

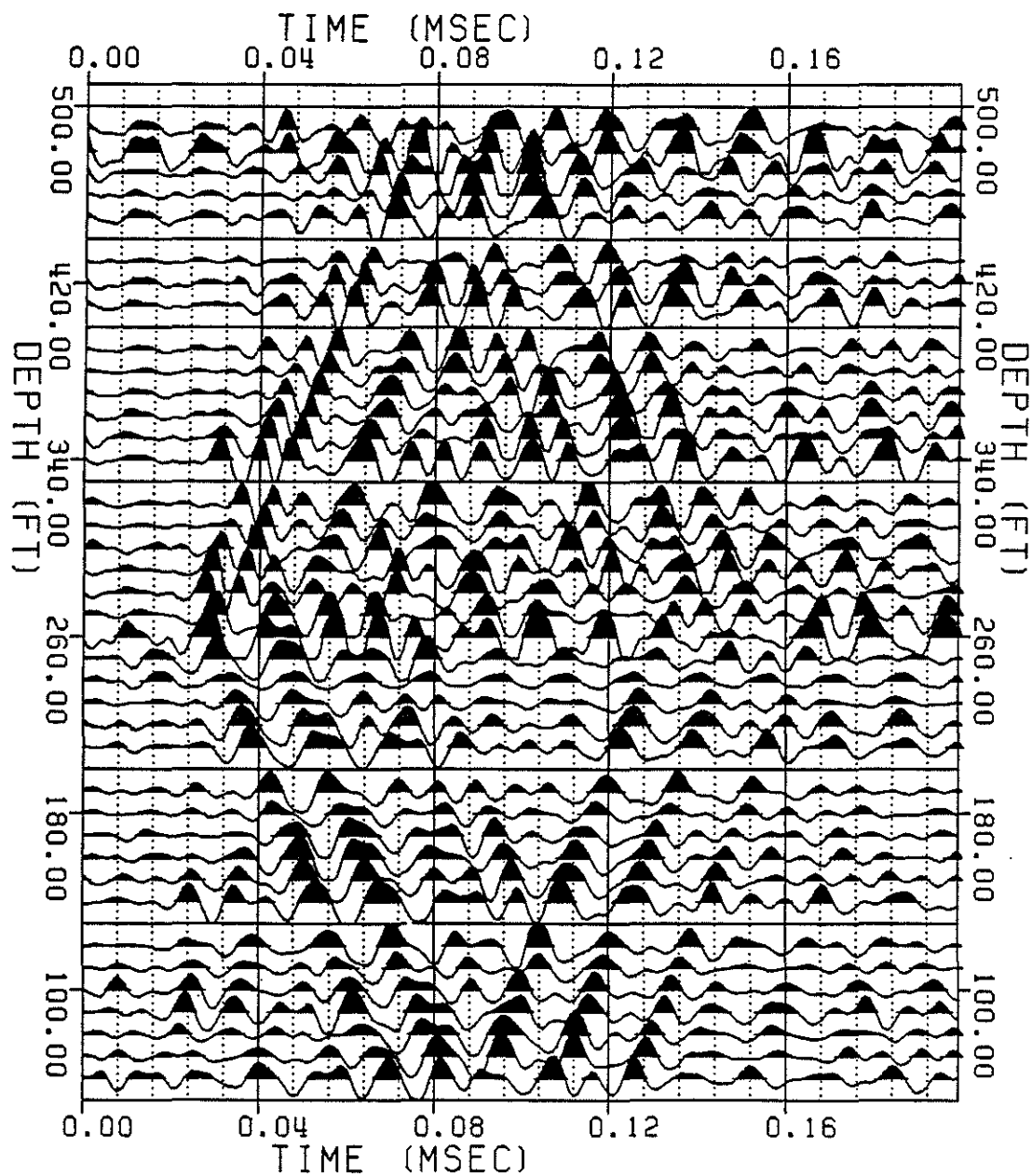


Figure 1: Example of fracture generated tube wave in a VSP, in Tyngsboro, Massachusetts.

BRITTON (HAMILTON) WELL No. 2
EXPLOSION SOURCE, OBSERVATION WELL
BANDPASS FILTERED (60 - 250 Hz)
TRACE AMPLITUDE NORMALIZATION

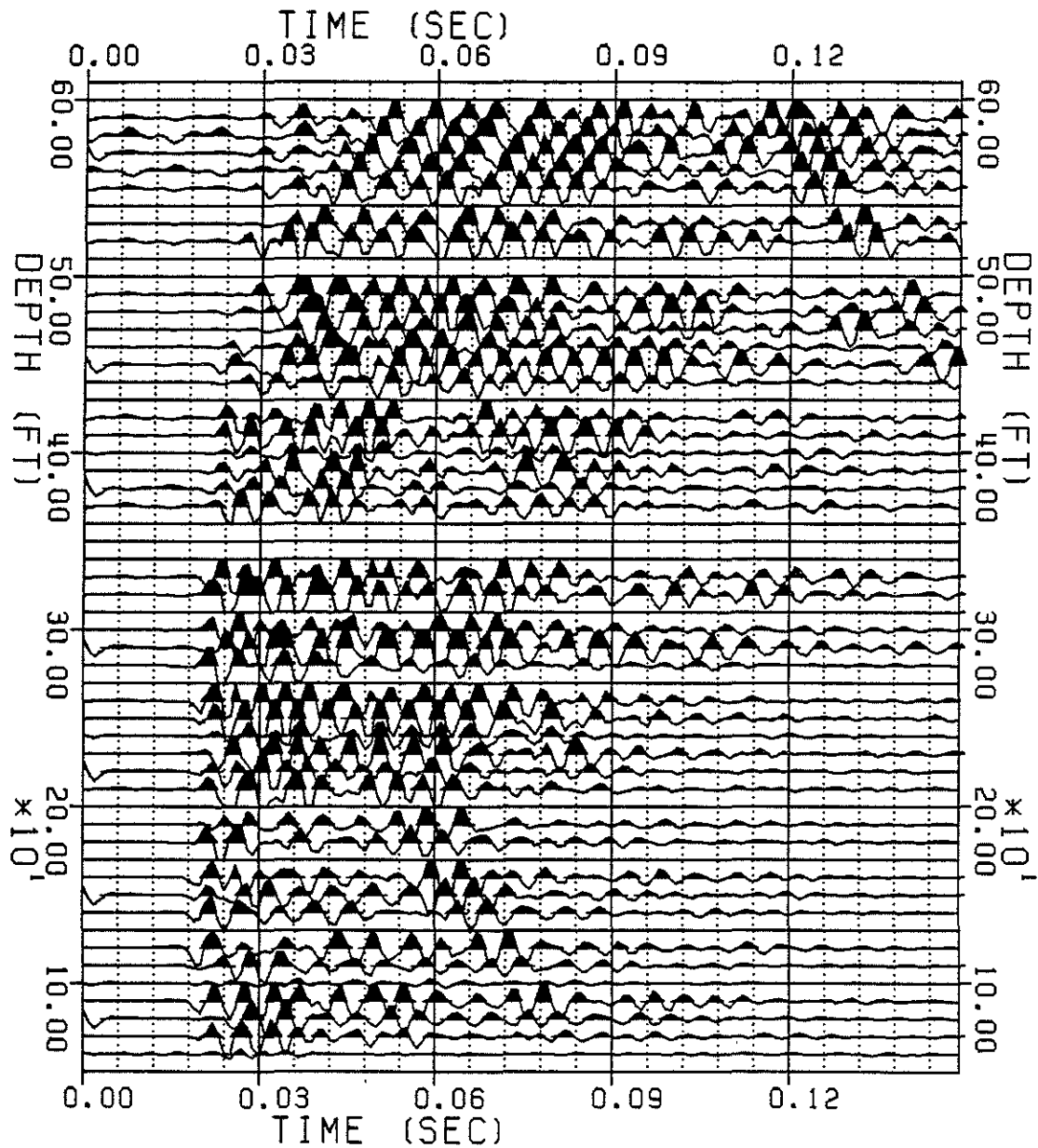


Figure 2: Example of fracture generated tube wave in a VSP, in Hamilton, Massachusetts.

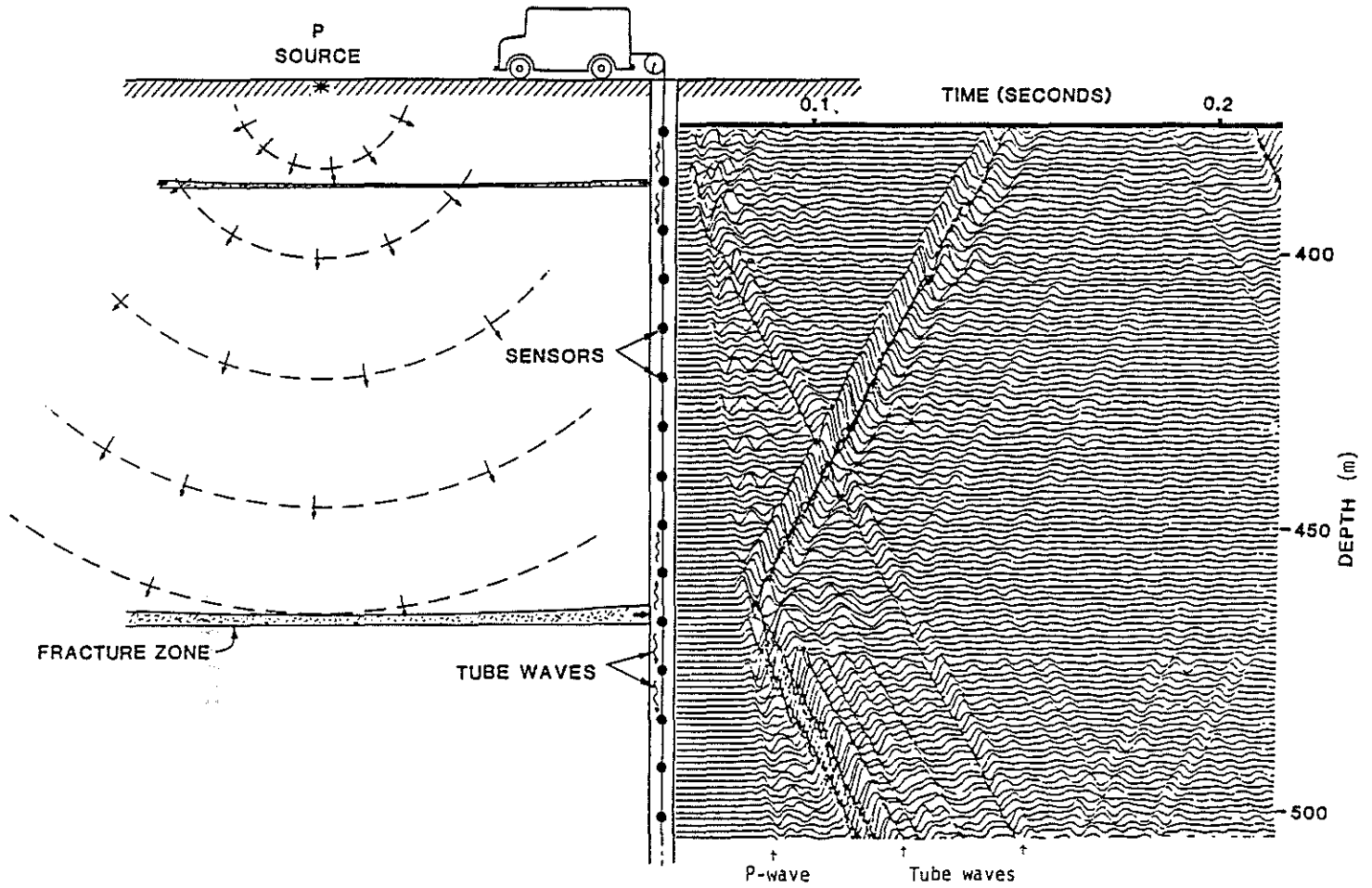


Figure 3: Schematic diagram of the mechanism of generation of tube waves (left) and an actual VSP section (from Huang & Hunter, 1981b) showing the fracture generated tube waves.

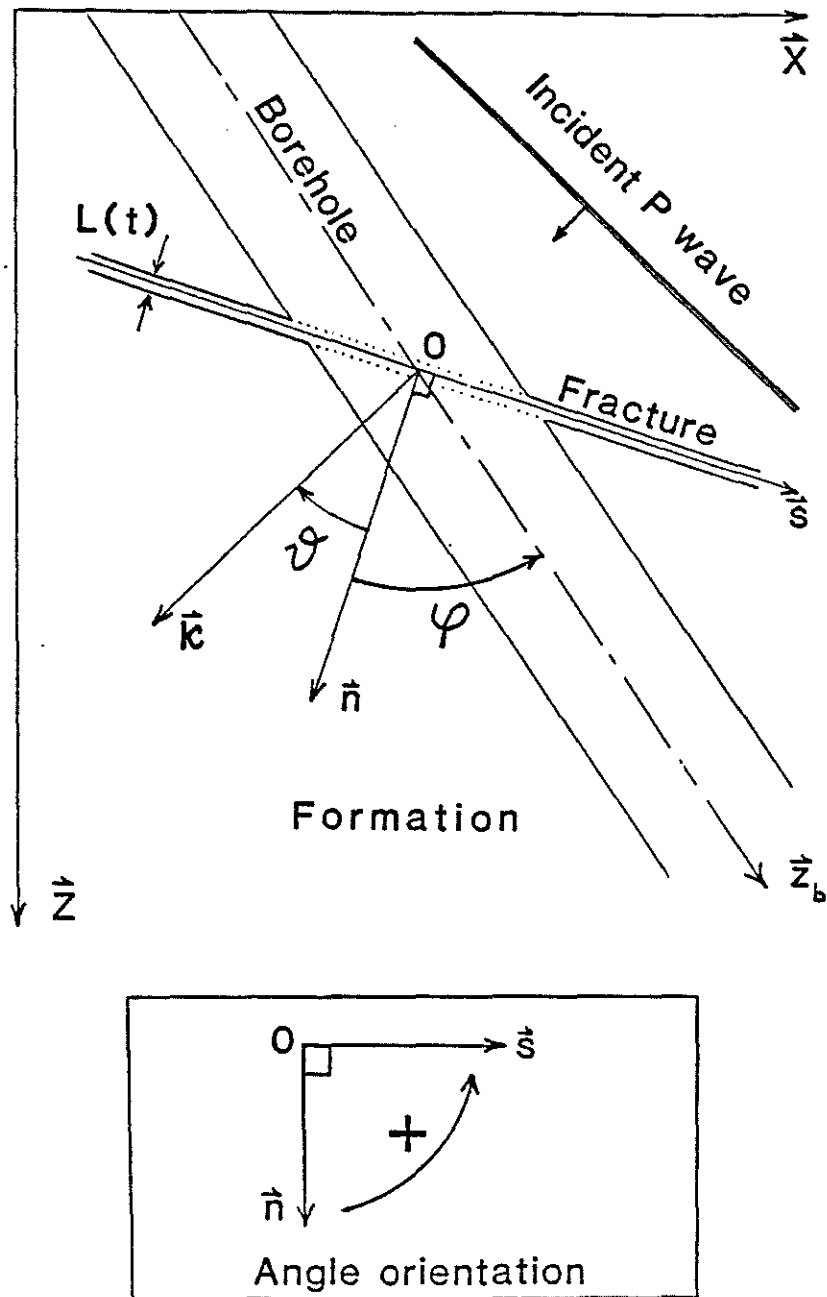


Figure 4: Fracture model used in this study

GRANITE FORMATION

FORMATION PARAMETERS

VP (M/S) =5500.
 VS (M/S) =3300.
 RHO (KG/M3) =2700.

FLUID PARAMETERS

VP (M/S) =1500.
 RHO (KG/M3) =1000.
 VISC. (PL) =0.0010
 INCOMP. (GPA) =2.00

BOREHOLE RADIUS (CM) =10.00

MIN-MAX TUBE WAVE VELOC. (M/S) =1446. - 1446.

BOT-TOP ISO-PERMEABILITIES (DARCY):

0.10 - 0.50 - 1.00 - 1.50 - 2.00

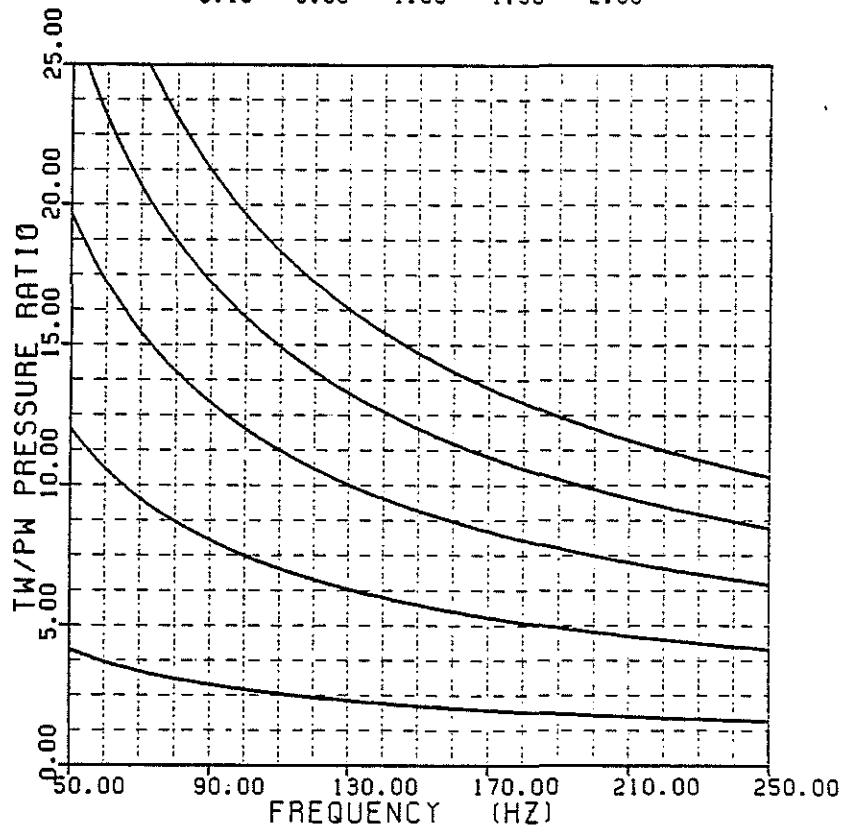


Figure 5a: Tube to P wave pressure ratios as functions of frequency and permeability in a granite.

GRANITE FORMATION

FORMATION PARAMETERS

VP (M/S) =5500.
 VS (M/S) =3300.
 RHO (KG/M3) =2700.

FLUID PARAMETERS

VP (M/S) =1500.
 RHO (KG/M3) =1000.
 VISC. (PL) =0.0010
 INCOMP. (GPA) =2.00

BOREHOLE RADIUS (CM) =10.00

MIN-MAX TUBE WAVE VELOC. (M/S) =1446. - 1446.

BOT-TOP ISO-PERMEABILITIES (DARCY):

0.10 - 0.50 - 1.00 - 1.50 - 2.00

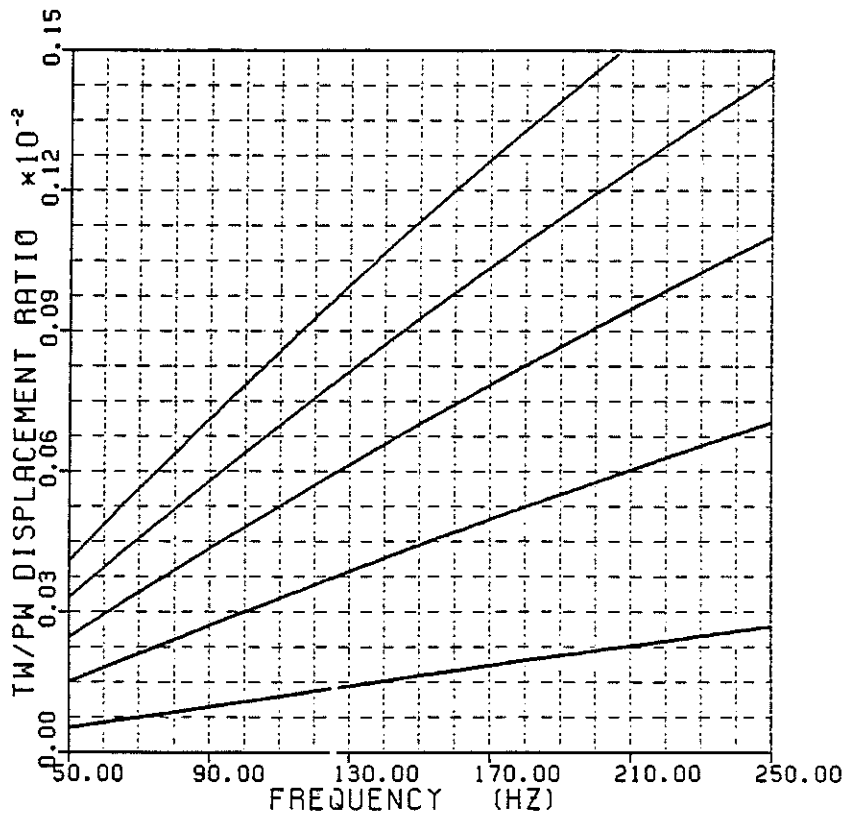


Figure 5b: Tube to P wave displacement ratios as functions of frequency and permeability in a granite.

HARD FORMATION

FORMATION PARAMETERS

VP (M/S) =4500.
 VS (M/S) =2500.
 RHO (KG/M3) =2300.

FLUID PARAMETERS

VP (M/S) =1500.
 RHO (KG/M3) =1000.
 VISC. (PL) =0.0010
 INCOMP. (GPA) =2.00

BOREHOLE RADIUS (CM) =10.00

MIN-MAX TUBE WAVE VELOC. (M/S) =1395. - 1395.

BOT-TOP ISO-PERMEABILITIES (DARCY):

0.10 - 1.00 - 2.00 - 4.00 - 6.00

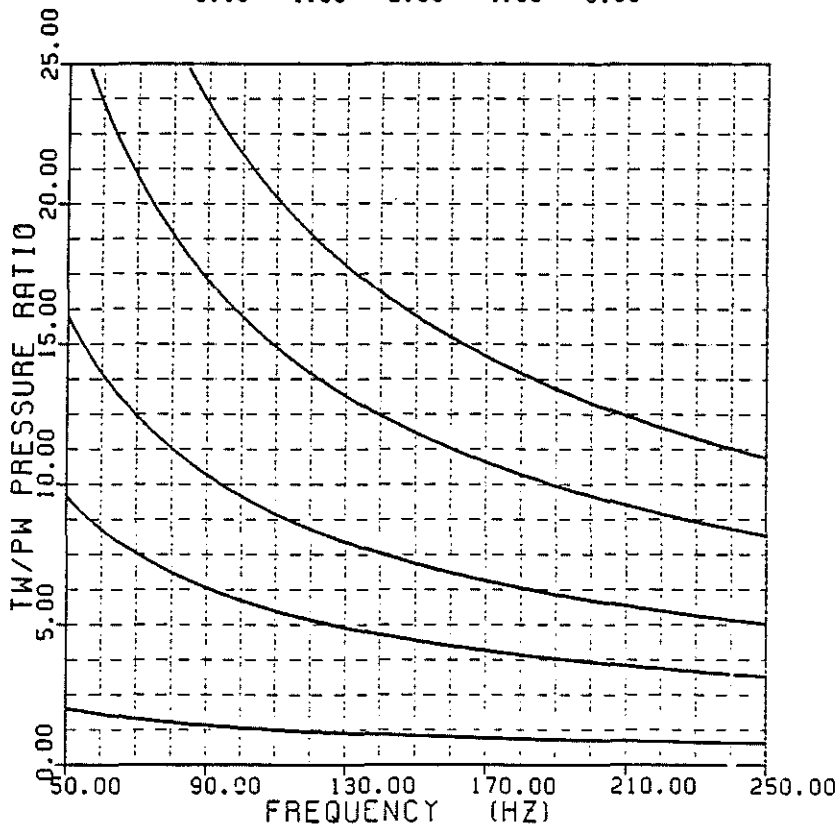


Figure 6a: Tube to P wave pressure ratios as functions of frequency and permeability in a "hard" formation.

HARD FORMATION

FORMATION PARAMETERS

VP (M/S) =4500.
 VS (M/S) =2500.
 RHO (KG/M3) =2300.

FLUID PARAMETERS

VP (M/S) =1500.
 RHO (KG/M3) =1000.
 VISC. (PL) =0.0010
 INCOMP. (GPA) =2.00

BOREHOLE RADIUS (CM) =10.00

MIN-MAX TUBE WAVE VELOC. (M/S) =1395. - 1395.

BOT-TOP ISO-PERMEABILITIES (DARCY):

0.10 - 1.00 - 2.00 - 4.00 - 6.00

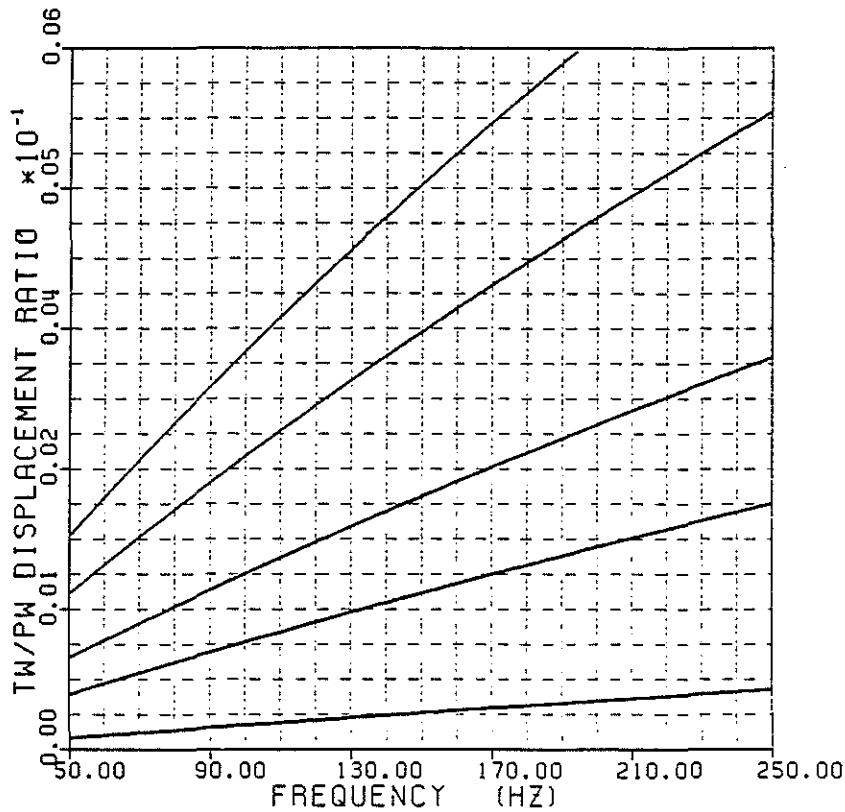


Figure 6b: Tube to P wave displacement ratios as functions of frequency and permeability in a "hard" formation.

SEDIMENT FORMATION

FORMATION PARAMETERS

VP (M/S) =3000.
 VS (M/S) =1200.
 RHO (KG/M3) =2100.

FLUID PARAMETERS

VP (M/S) =1500.
 RHO (KG/M3) =1000.
 VISC. (PL) =0.0010
 INCOMP. (GPA) =2.00

BOREHOLE RADIUS (CM) =10.00
 MIN-MAX TUBE WAVE VELOC. (M/S) =1136. - 1132.
 BOT-TOP ISO-PERMEABILITIES (DARCY):
 1.00 - 5.00 - 10.00 - 15.00 - 20.00

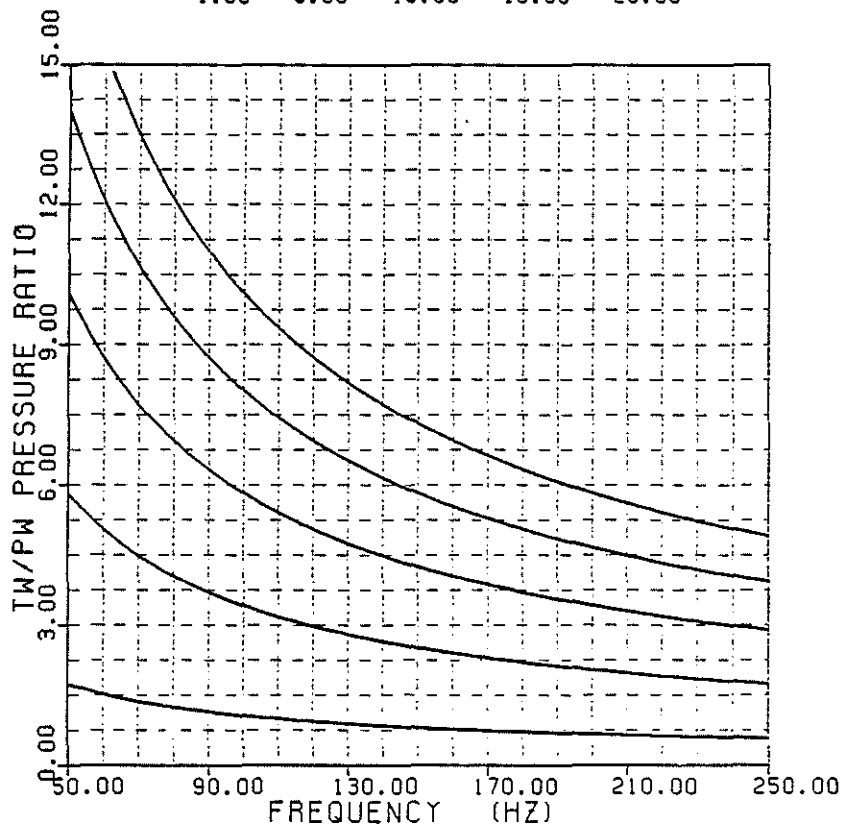


Figure 7a: Tube to P wave pressure ratios as functions of frequency and permeability in a "sediment."

SEDIMENT FORMATION

FORMATION PARAMETERS

VP (M/S) =3000.

VS (M/S) =1200.

RHO (KG/M3) =2100.

FLUID PARAMETERS

VP (M/S) =1500.

RHO (KG/M3) =1000.

VISC. (PL) =0.0010

INCOMP. (GPA) =2.00

BOREHOLE RADIUS (CM) =10.00

MIN-MAX TUBE WAVE VELOC. (M/S) =1136. - 1132.

BOT-TOP ISO-PERMEABILITIES (DARCY):

1.00 - 5.00 - 10.00 - 15.00 - 20.00

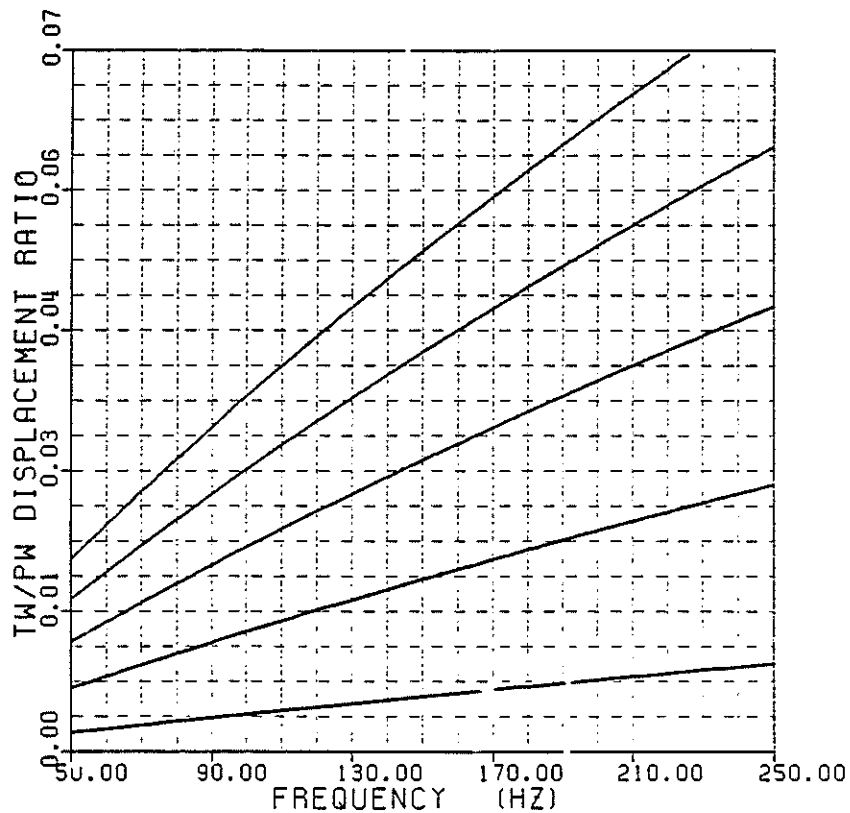


Figure 7b: Tube to P wave displacement ratios as functions of frequency and permeability in a "sediment."

HARD FORMATION

FORMATION PARAMETERS

VP (M/S) =4500.
 VS (M/S) =2500.
 RHO (KG/M3) =2300.

FLUID PARAMETERS

VP (M/S) =1500.
 RHO (KG/M3) =1000.
 VISC. (PL) =0.0010
 INCOMP. (GPA) =2.00

F R E Q U E N C Y (HZ) =150.

TUBE WAVE VELOCITY (M/S) =1395.

BOT-TOP ISO-PERMEABILITIES (DARCY):

0.10 - 1.00 - 2.00 - 4.00 - 6.00

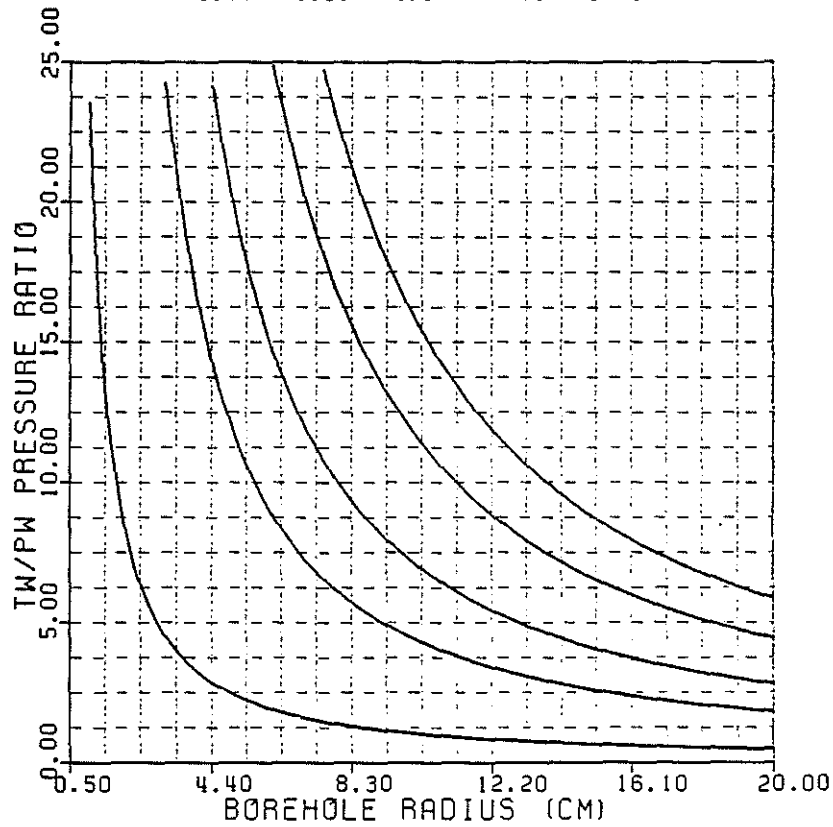


Figure 8: Tube to P wave pressure ratios as functions of borehole radius and permeability in a "hard" formation.

GRANITE FORMATION

FORMATION PARAMETERS

VP (M/S) =5800.
 VS (M/S) =3300.
 RHO (KG/M3) =2700.

FLUID PARAMETERS

VP (M/S) =1500.
 RHO (KG/M3) =1000.
 VISC. (PL) =0.0010
 INCOMP. (GPA) =2.00

BOREHOLE RADIUS (CM) =7.60
 MIN-MAX TUBE WAVE VELOC. (M/S) =1446. - 1446.
 BOT-TOP ISO-PERMEABILITIES (DARCY):
 0.10 - 0.20 - 0.50 - 1.00 - 2.00

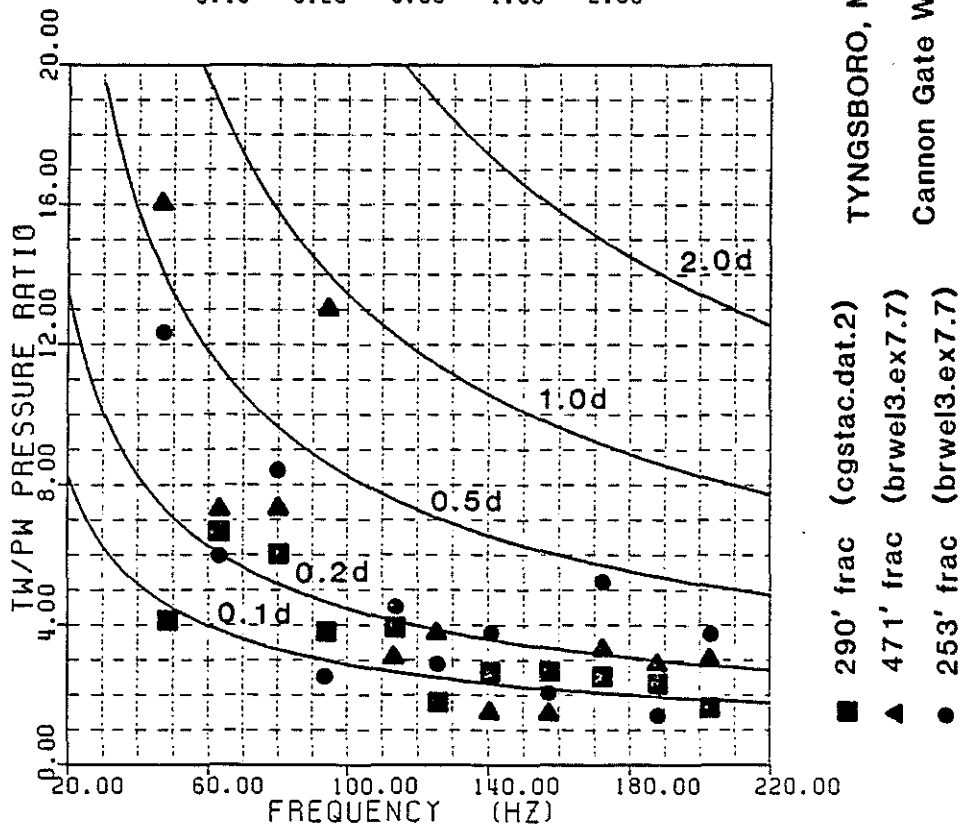


Figure 9: Data versus theoretical tube to P wave pressure ratios as functions of frequency and permeability in a granite.